EVIDENCE OF INTERVALLEY SCATTERING OF ELECTRONS IN THE EXTRINSIC PHOTOCONDUCTIVITY OF n-TYPE SILICON

A. Onton
IBM Watson Research Center, Yorktown Heights, New York
(Received 10 January 1969)

The extrinsic photoconductivity of n-type silicon has revealed dips in its spectral response due to transfer of electrons among the equivalent conduction-band valleys by intervalley phonon emission. Intervalley LA phonons of energy 26.9 and 47.4 meV (±0.5 meV) are observed to contribute approximately equally to the total scattering of electrons.

Stocker[1] has suggested the possibility of observing electron-phonon umklapp processes in the photoconductive response of multivalleyed n-type semiconductors. He predicts that dips in the extrinsic photoconductive spectral response should occur at intervalley-phonon-emission threshold energies. Present experiments at liquid helium temperatures using silicon doped with antimony, phosphorus, or arsenic reveal dips in the photoconductive spectral response that are consistent with intervalley scattering by phonons of 26.9 and 47.4 meV (±0.5 meV) in energy.

The present effect is the analog, in a multivalleyed semiconductor, of the oscillatory photoconductivity observed in a number of direct-gap semiconductors. In InSb,[2,3] GaSb,[3] ZnTe,[4] GaAs,[5] and CdS,[6] oscillatory intrinsic photoconductivity has been observed due to energy loss by electrons through intraband LO-phonon emission—a process not very probable in silicon. In p-type Ge,[7] oscillatory extrinsic photoconductivity has been ascribed to the variation of optical transition probability with emission of zone-center phonons.

Data on which the present results are based are shown in Fig. 1. The figure shows the relative photoconductive spectral response per incident photon for silicon with phosphorus [Si(P)] or antimony [Si(Sb)] donors. The spectra were obtained using a prism monochromator with a KBr or NaCl prism. The dips in photoconductivity significant for this Letter are indicated by A, B, and C. The other structure is due to light lost to competing absorption mechanisms such as lattice vibrations and local modes.[8] For example, the decrease in photoconductive response near 140 meV is due to local modes of oxygen in silicon.[9] With Si(Sb) the photoconductivity dips A, B, and C are observed at lower energy than the corresponding dips with Si(P).

The occurrence of photoconductivity dips due to scattering of electrons by phonons other than low-energy acoustic modes can be understood as follows. No photocurrent is observed until the photon energy, $h\nu$, exceeds the ionization energy for the donor electron, ϵ_i. For higher photon energies, the photocurrent is observed to increase with photon energy. This is primarily because the electron lifetime, with respect to capture by an ionized donor, increases as the electron becomes more energetic. However, when the incident photon energy satisfies

$$h\nu = \epsilon_i + nh\omega_j, \quad n = 1, 2, 3, \cdots, \tag{1}$$

where $h\omega_j$ are the energies of phonons that can scatter the electron, it is possible for electrons injected at these energies to decay rapidly to states near the bottom of the conduction band via phonon emission. The resulting decrease in average lifetime of electrons should be observable in the photoconductive spectral response as dips at photon energies satisfying Eq. (1). A shift of the phonon-emission dips with donor ionization energy is expected on the basis of Eq. (1), and is indeed observed.

Table I lists the positions of the photoconductiv-

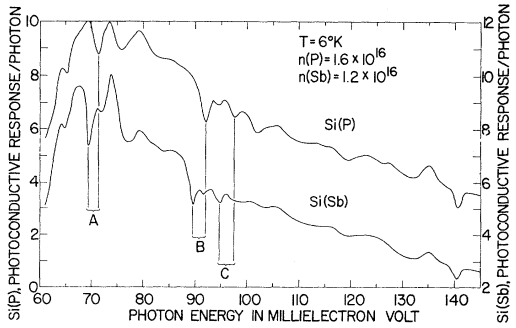

FIG. 1. Relative photoconductive response per photon as a function of incident photon energy for silicon doped with antimony or phosphorus. The curve for Si(Sb) has been displaced for graphic clarity. The dc electric field in the samples was estimated to be approximately 65 V/cm, the voltage drop in the broad-area nickel-plate contacts being assumed to be small.

Table I. Positions of dips in photoconductivity in meV.

Dip	Si(Sb), $\epsilon_i = 42.2$		Si(P), $\epsilon_i = 45.0$		Si(As), $\epsilon_i = 53.2$		Average
	$h\nu$	$h\nu-\epsilon_i$	$h\nu$	$h\nu-\epsilon_i$	$h\nu$	$h\nu-\epsilon_i$	$h\nu-\epsilon_i$
A	69.4	27.2	71.5	26.5	80.1	26.9	26.9
B	89.6	47.4	92.0	47.0	100.9	47.7	47.4
C	94.7	52.5	97.5	52.5	106.5	53.3	52.8

ity dips *A*, *B*, and *C* as observed with antimony-, phosphorus-, or arsenic-doped silicon. Also given are the optical ionization energies of the donors obtained by adding the binding energy of the $2p(m=\pm1)$ electron state calculated by Kohn and Luttinger[10] to the energy required for the $1S(A_1) \rightarrow 2p_\pm$ transition as observed by Aggarwal and Ramdas.[11,12] The difference, $h\nu-\epsilon_i$, gives the energy carried away by the emitted phonon. Within an experimental uncertainty of about ±0.5 meV, the averaged results in Table I indicate that phonons of 26.9 and 47.4 meV are involved. The dip *C* is believed to be caused by the consecutive emission of two 26.9-meV phonons. These phonon energies are consistent with the energies of the intervalley phonons determined by Dumke[13] on the basis of low-temperature recombination radiation spectra of silicon obtained by Haynes. The interpretation for these phonons remains as suggested by Dumke except for small changes in numerical values; i.e., the 26.9-meV phonon is an LA phonon with wave vector $(0.42, 0, 0)2\pi/a$ and the 47.4-meV phonon an LA phonon with wave vector $(1, 0.21, 0.21)2\pi/a$. These phonons participate in *g* scattering (transfer of an electron between the valley along [100] and the equivalent [$\bar{1}$00] valley) and *f* scattering (electron transfer from the valley along [100] to one of the four valleys along [010], [0$\bar{1}$0], [001], or [00$\bar{1}$]), respectively. The wave vectors have been deduced using the data of Brockhouse[14] on the vibrational spectrum of silicon, and suggest that the conduction-band minima in silicon lie at $\vec{k} = \langle 0.79, 0, 0\rangle$.

There is no evidence in the photoconductivity data of structure corresponding to intraband scattering by LO phonons at $h\nu = \epsilon_i + 64$ meV. This is consistent with the conclusion by Dumke[6] that intervalley scattering and intravalley scattering by acoustic modes can account for nearly all of the scattering of electrons in silicon.

The relative magnitudes of the photoconductivity dips corresponding to *g* and *f* scattering, divided by the respective total photoconductive responses at those points, give the approximate relative magnitudes of the coupling coefficients for these two scattering processes. The ratio of these total scattering coupling coefficients is found to be near unity:

$$\omega_g/\omega_f = 1.0 \pm 0.4.$$

This ratio can be compared with Dumke's[13] result of about 2.5 and Long's[15] value of 0.075 for the same ratio. The present results indicate that *g* scattering in silicon is somewhat less efficient relative to *f* scattering than estimated by Dumke but much more efficient than deduced by Long on the basis of the temperature dependence of conductivity, Hall effect, and weak-field magnetoresistance measurements. At least in part, the discrepancy with Long's results can be explained on the basis of the intervalley phonon energies assumed by him: 16.5 and 55 meV.

The author would like to acknowledge helpful discussions with W. P. Dumke and the assistance of R. E. Fern and V. Garrison in the experimental work.

[1]H. J. Stocker, Solid State Commun. 6, 125 (1968).
[2]H. J. Stocker, H. Levinstein, and C. R. Stannard, Jr., Phys. Rev. 150, 613 (1966).
[3]M. A. Habegger and H. Y. Fan, Phys. Rev. Letters 12, 99 (1964).
[4]R. E. Nahory and H. Y. Fan, Phys. Rev. Letters 17, 251 (1966).
[5]R. E. Nahory, Phys. Rev. (to be published).
[6]Y. S. Park and D. W. Langer, Phys. Rev. Letters 13, 392 (1964).
[7]C. Benoit à la Guillaume and J. Cernogora, J. Phys. Chem. Solids 24, 383 (1963).
[8]E. Burstein, J. J. Oberly, and J. W. Davisson, Phys. Rev. 89, 331 (1953).
[9]H. J. Hrostowski and R. H. Kaiser, Phys. Rev. 107, 966 (1957).
[10]W. Kohn and J. M. Luttinger, Phys. Rev. 98, 915 (1955).
[11]R. L. Aggarwal and A. K. Ramdas, Phys. Rev. 137,

A602 (1965).
[12]R. L. Aggarwal, thesis, Purdue University, 1965 (unpublished).
[13]W. P. Dumke, Phys. Rev. 118, 938 (1960). A reanalysis of the data reported in this paper shows that a 27-meV phonon gives better consistency with the data than the 23-meV value reported: W. P. Dumke, private communication.
[14]B. N. Brockhouse, Phys. Rev. Letters 2, 256 (1959).
[15]D. Long, Phys. Rev. 120, 2024 (1960).

SPIN WAVES AND THE ORDER-DISORDER TRANSITION IN CHROMIUM

J. Als-Nielsen and O. W. Dietrich
Danish Atomic Energy Commission Research Establishment Risö, Roskilde, Denmark
(Received 16 December 1968)

The inelastic magnetic scattering of neutrons has been studied in Cr and $Cr_{0.95}$-$Mn_{0.05}$ both below and above the Néel temperature. The temperature dependence of the spin-wave velocity in the alloy has been measured below T_N. The scattering above T_N may also be interpreted in terms of spin-wavelike excitations, which persist far into the paramagnetic phase.

Using a triple-axis spectrometer, we have studied the inelastic magnetic scattering of neutrons in single crystals of Cr and $Cr_{0.95}$-$Mn_{0.05}$ both below and above the Néel temperature T_N. The addition of 5% Mn to Cr causes the spin-density wavelength to become commensurable with the lattice periodicity so that a simple antiferromagnetic structure results.[1] This simplifies the study of the magnetic excitations, and most of the measurements presented in this paper were therefore performed on the alloy.

The inelastic neutron scattering observed in $\vec{q}$ scans for constant energy transfer $\hbar\omega$ at room temperature in the alloy is shown in the left of Fig. 1, $\vec{q}$ being the distance of the scattering vector from (1, 0, 0), which is a point of the magnetic superlattice in reciprocal space. This scattering is interpreted as being of magnetic origin for the following reasons: (i) No peak was observed in $\vec{q}$ scans through the nonsuperlattice point (1, 1, 0). (ii) A $\vec{q}$ scan at 10 meV through the (1, 1, 1) superlattice point yielded a width consistent with those of Fig. 1. (iii) $\vec{q}$ scans through (1, 0, 0) with different spectrometer settings, using various combinations of Be(0, 0, 2), Zn(0, 0, 2), and Ge(1, 1, 1) as monochromator and analyzer planes, all gave widths consistent with those of Fig. 1. (iv) The pronounced temperature dependence of scans at 10 meV through (1, 0, 0), shown in the lower part of Fig. 1, is strong evidence that the scattering is of magnetic origin.

The magnetic excitations in an itinerant antiferromagnet have been discussed by Fedders and Martin[2] and have the form of spin waves with a linear dispersion relation at small wave vectors. We have therefore interpreted our data in terms of undamped spin waves with a scattering cross section of the form $S(\vec{q}, \omega) \sim \delta(\omega - c|\vec{q}|)$. Because of the limited resolution of the spectrometer, the peak around (1, 0, 0) is composed of unresolved contributions from spin waves propagating in all directions. In principle it might be possible to resolve these contributions by using larger scattering vectors, e.g., around the (1, 1, 1) reflection, but in practice the decrease in the form factor[3] results in impracticably low intensities. The interpretation of the results therefore depends upon a very careful treatment of the experimental resolution. The intensity $I(\vec{q}^0, \omega^0)$ at the spectrometer setting $(\vec{q}^0, \omega^0)$ is the convolution of the experimental resolution function $R(\vec{q}, \omega)$ and $S(\vec{q}, \omega)$, so that

$$I(\vec{q}^0, \omega^0) \propto \int R(\vec{q}-\vec{q}^0, \omega-\omega^0) S(\vec{q}, \omega) d^3q d\omega. \quad (1)$$

We have assumed that the angular distributions of the mosaic blocks in the crystals and the collimator transfer functions may be approximated by Gaussians, and that the component q_z normal to the scattering plane is uncorrelated with the other variables. If we now approximate the cone dispersion surface by a cylinder within the range of the resolution function, and use the fact that the resolution width in the direction of q_z is much greater than ω^0/c, we find

$$I(q_x^0, 0, 0, \omega^0) \propto \int_{q_x^2+q_y^2=0}^{(\omega^0/c)^2} \left[\left(\frac{\omega^0}{c}\right)^2 - q_x^2 - q_y^2\right]^{-1/2} \exp\left[-\frac{(q_x-q_x^0)^2}{\sigma_x^2} - \frac{q_y^2}{\sigma_y^2} - k(q_x-q_x^0)q_y\right] dq_x dq_y, \quad (2)$$